Accepted Manuscript

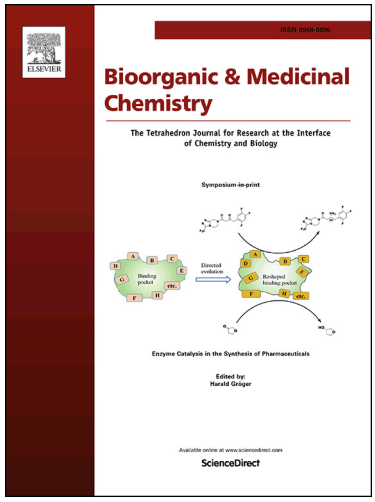

Design, synthesis,in vitro and in vivo evaluation, and structure-activity relationship (SAR) discussion of novel dipeptidylboronicacidproteasome inhibitors as orally available anti-cancer agents for the treatment of multiple myeloma and mechanism studies

Meng Lei, Huayun Feng, Enhe Bai, Hui Zhou, Jia Wang, Jingmiao Shi, Xueyuan Wang, Shihe Hu, Zhaogang Liu, Yongqiang Zhu

PII: S0968-0896(18)30521-2
DOI: https://doi.org/10.1016/j.bmc.2018.06.020
Reference: BMC 14412

To appear in: *Bioorganic & Medicinal Chemistry*

Received Date: 14 March 2018
Revised Date: 11 June 2018
Accepted Date: 14 June 2018

Please cite this article as: Lei, M., Feng, H., Bai, E., Zhou, H., Wang, J., Shi, J., Wang, X., Hu, S., Liu, Z., Zhu, Y., Design, synthesis,in vitro and in vivo evaluation, and structure-activity relationship (SAR) discussion of novel dipeptidylboronicacidproteasome inhibitors as orally available anti-cancer agents for the treatment of multiple myeloma and mechanism studies, *Bioorganic & Medicinal Chemistry* (2018), doi: https://doi.org/10.1016/j.bmc.2018.06.020

Design, synthesis, in vitro and in vivo evaluation, and structure-activity relationship (SAR) discussion of novel dipeptidyl boronic acid proteasome inhibitors as orally available anti-cancer agents for the treatment of multiple myeloma and mechanism studies

Meng Lei [a, 1], Huayun Feng [a, 1], Enhe Bai [b], Hui Zhou [b], Jia Wang [c], Jingmiao Shi [c], Xueyuan Wang [b], Shihe Hu [c, *], Zhaogang Liu [c], Yongqiang Zhu [b, *]

[a] *College of Science, Nanjing Forestry University, No. 159 Longpan Road, Nanjing 210037, PR China*

[b] *College of Life Science, Nanjing Normal University, No. 1 Wenyuan Road, Nanjing 210037, PR China*

[c] *Jiangsu Chia Tai Fenghai Pharmaceutical Co. Ltd., No. 9 Weidi Road, Nanjing 210046, PR China*

Abstract

A series of novel dipeptidyl boronic acid inhibitors of 20S proteasome were designed and synthesized. Aliphatic groups at R^1 position were designed for the first time to fully understand the SAR (structure-activity relationship). Among the screened compounds, novel inhibitor **5c** inhibited the CT-L (chymotrypsin-like) activity with IC_{50} of 8.21 nM and the MM (multiple myeloma) cells RPMI8226, U266B and ARH77 proliferations with the IC_{50} of 8.99, 6.75 and 9.10 nM, respectively, which showed similar in vitro activities compared with the compound **MLN2238** (biologically active form of marketed **MLN9708**). To investigate the oral availability, compound **5c** was esterified to its prodrug **6a** with the enzymatic IC_{50} of 6.74 nM and RPMI8226, U266B and ARH77 cell proliferations IC_{50} of 2.59, 4.32 and 3.68 nM, respectively. Furthermore, prodrug **6a** exhibited good pharmacokinetic properties with oral bioavailability of 24.9%, similar with **MLN9708** (27.8%). Moreover, compound **6a** showed good microsomal stabilities and displayed stronger in vivo anticancer efficacy than **MLN9708** in the human ARH77 xenograft mouse model. Finally, cell cycle results showed that compound **6a** had a significant inhibitory effect on CT-L and inhibited cell cycle progression at the G2M stage.

Keywords: Dipeptidyl boronic acid; Proteasome; Pharmacokinetic; Cell cycle; Xenograft mouse model

---

[1] These authors contributed equally to the work

Tel.:+86 25 85891591.

E-mail address: zhyqscu@hotmail.com (Y.Q. Zhu)

Tel.:+86 25 57033246-8280.

E-mail address: hsh.2@163.com (S.H. Hu)

1. Introduction

The ubiquitin-proteasome pathway (UPP) plays a major role in cellular protein degradation process and more than 80% proteins are degraded by this pathway in eukaryotic cells.[1] It has been shown that the pathway is involved in many physiologically important cellular processes, including cell cycle progression, transcriptional regulation, signal transduction, DNA repair, antigen presentation and immune response.[2-4]

Proteasome is a multi-catalytic protease complex responsible for protein degradation in eukaryotes, composed of one multicatalytic proteinase complex referred to as the 20S proteasome core particle (CP) and two regulatory particles 19S proteasome (RP). The 19S regulatory particle is responsible for recognition and unfolding. Ubiquited proteins are translocated into the active sites of the 20S proteasome and digested into small peptides.[5-7] There are three active β subunits in the 20S proteasome, β1, β2 and β5, which are responsible for the caspase-like (C-L), trypsin-like (T-L) and chymotrypsin-like (CT-L) activities, respectively.[8]

This pathway has an important relationship with cardiovascular disease,[9] cancer,[10] neurodegenerative diseases[11] and so on. The potent and selective dipeptide boronic acid proteasome inhibitor **bortezomib** (PS341, Figure 1), was approved by FDA for treatment of multiple myeloma (MM) and mantle cell lymphoma (MCL).[12-16] However, **bortezomib** was only intravenously or subcutaneously administered, which gave patients great inconvenience. **MLN9708** (Figure 1) is the second generation of small molecule proteasome inhibitor, which has a shorter proteasome dissociation half-life,[17-19] as well as improved pharmacokinetics, pharmacodynamics, and superior antitumor activity in xenograft models and solid tumor compared with **bortezomib**. Furthermore, **MLN9708** is an orally bioavailable proteasome inhibitor and shows effective at various regimens and dosing routes.[20] **MLN9708** rapidly hydrolyzes to its biologically active form **MLN2238** (Figure 1) in aqueous solutions or plasma.

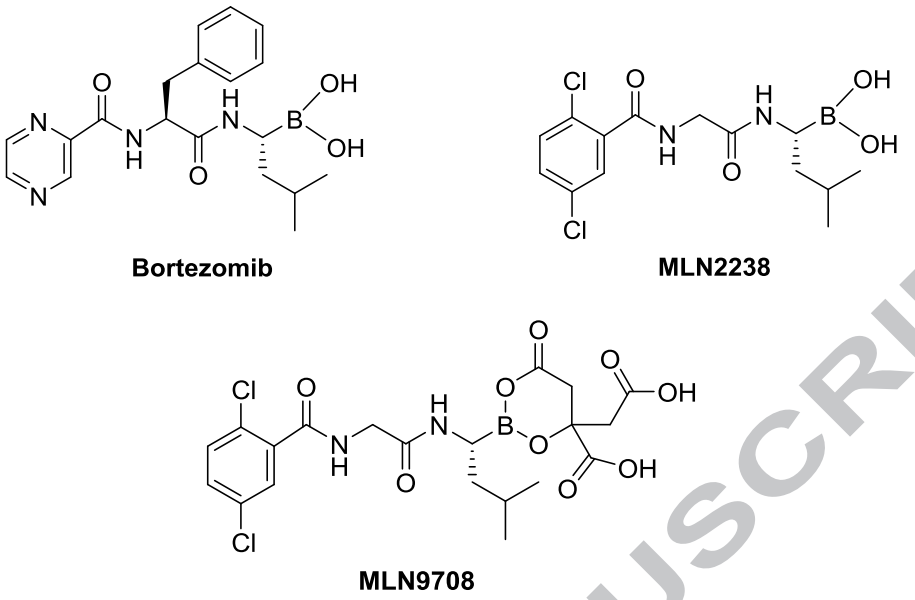

Figure 1. Structures of dipeptidyl boronic acid proteasome inhibitors approved by FDA.

Although the administration of **MLN9708** was changed, it also gave patients a powerful dose of side effects and a low association with neuropathy.[20] So there is a great need to design and develop novel orally bioavailable molecules with low toxicity. In our previous work, many aromatic groups at R^1 position were designed to discuss the SAR.[22-26] However, aliphatic groups had never been studied. In this manuscript, several aliphatic groups including straight chain and cyclic groups were synthesized, biologically investigated to fully understand the SAR. To improve the metabolic stabilities, aliphatic groups were also designed at R^2 position and SAR was discussed. Finally, the compound with improved activity was synthesized to its oral prodrug to improve the mode of administration.

2. Results and discussion

2.1. Chemistry

The synthesis of final compounds **5a-5v** and **6a** was illustrated in Scheme 1. *N*-terminal protected amino acids of **1a-1c** reacted with the commercially available amino boronate trifluoroacetate **2** using the coupling synthesis method to afford the dipeptidyl boronic acid esters. Then *N*-terminal protected groups were removed with HCl in ethyl acetate to form boronic acid ester hydrochlorides **3a-3c** (yields 66.2-80.6%). The key intermediates **3a-3c** were coupled with various acids R^1COOH in the presence of EDCI and HOBt to afford the corresponding peptide esters **4a-4e**

(yields 41.8-80.8%), while various acyl chloride R^1COCl reacted with **3a-3c** in the presence of triethylamine (Et_3N) to obtain the corresponding peptide esters **4f-4v** (yield 39.7-95.1%). Finally, after transesterification of esters **4a-4v** with isobutylboronic acid, target compounds **5a-5v** were obtained in moderate to high yields (31.3-86.4%). Dipeptidyl boronic acid **5c** then reacted with diethanolamine to afford the corresponding prodrug **6a** (yield 65.6%). The structures of the target compounds were displayed in Table 1.

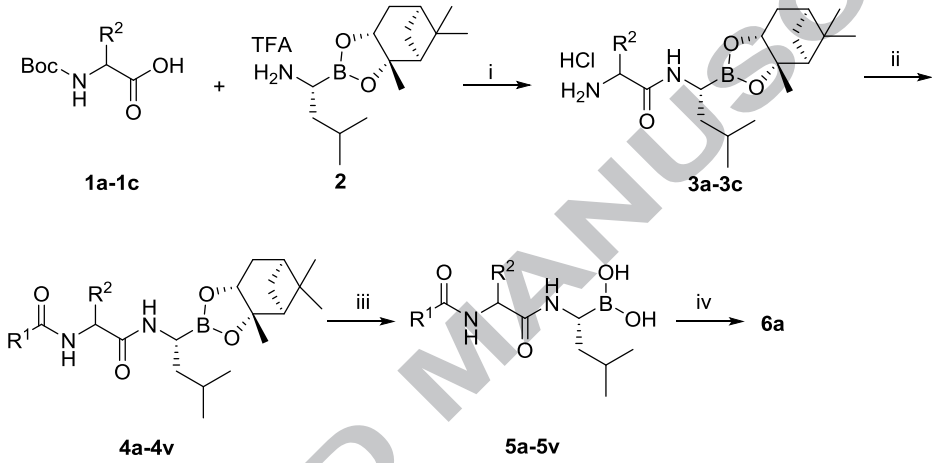

Scheme 1. General Synthesis of Dipeptidyl Boronic Acids **5a-5v** and Prodrug **6a**. Reagents and conditions: (i) (1) EDCI, HOBt, DIPEA, CH_2Cl_2, -10 °C to rt; (2) HCl in ethyl acetate, CH_2Cl_2, -5 °C to rt; (ii) R^1COOH, EDCI, HOBt, DIPEA, CH_2Cl_2, -10 °C to rt; or R^1COCl, Et_3N, CH_2Cl_2, -15 °C to rt; (iii) 1 N HCl, MeOH, hexane, rt. (iv) ethyl acetate, 74 °C to rt.

2.2 Biological evaluation

2.2.1 Enzyme

The capacities of target compounds to inhibit the CT-L activity of β5 subunit of 20S human proteasome were assayed using appropriate fluorogenic substrates. And part compounds were also assayed the activities against β1 and β2 subunits. The marketed **bortezomib**, **MLN2238** and **MLN9708** were used as the standards. The IC_{50} values of compounds **5a-5v, 6a**, **bortezomib**, **MLN2238** and **MLN9708** were shown in Table 1.

Table 1

Structures of compounds **5a-5v, 6a**, **Bortezomib**, **MLN2238**, **MLN9708** and their proteasome inhibitory activities

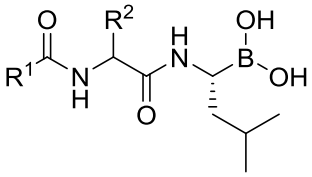

Compd.	R^1	R^2	$^aIC_{50}$ (nM)
5a	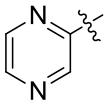		74.86
5b	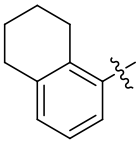		4.82
5c	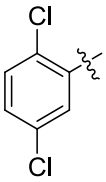		8.21
5d	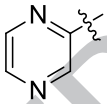	H	303.80
5e	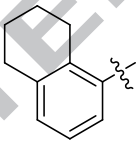	H	5.89
5f		H	387
5g	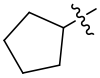	H	21.17
5h	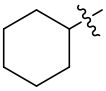	H	12.89
5i		H	593.70
5j	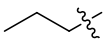	H	42.79
5k	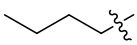	H	30.78
5l	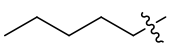	H	27.75
5m	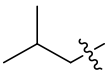	H	20.44

5n	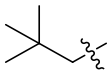	H	26.79
5o		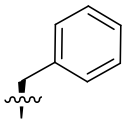	8.11
5p	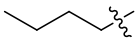	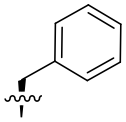	3.53
5q	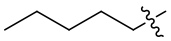	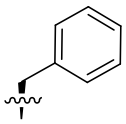	2.31
5r	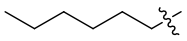	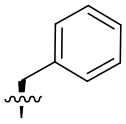	1.98
5s	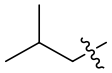	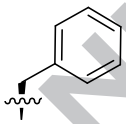	4.16
5t		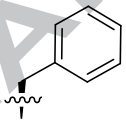	8.86
5u		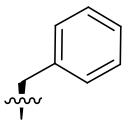	5.26
5v		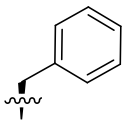	3.22
6a	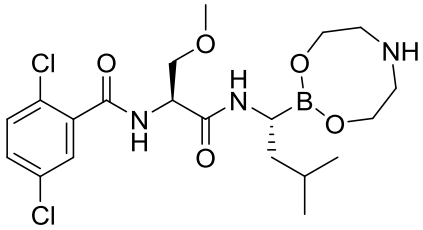		6.74 (12.98[b], 1442[c])
Bortezomib	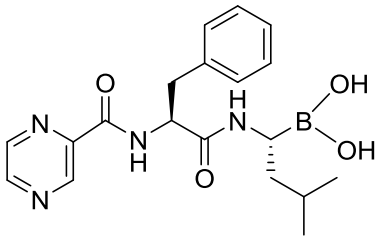		7.04 (96.5[b], 3998 [c])
MLN2238	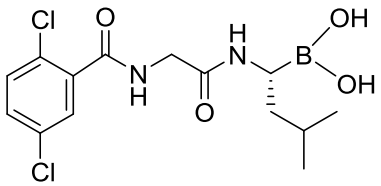		7.73

MLN9708	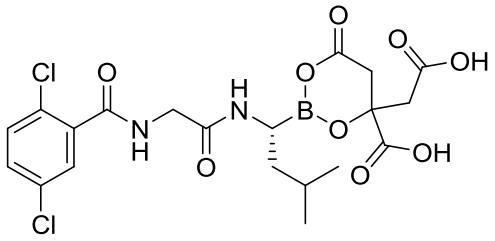	8.44 (10.64[b], 7954[c])

[a] IC_{50} value obtained for **bortezomib**, **MLN2238** and **MLN9708** under our experimental conditions. [b,c] IC_{50} values for the inhibition of β1 and β2 subunits.

Pyrazin-2-yl and 2,5-dichlorobenz-yl groups were the building blocks of marketed **bortezomib** and **MLN9708** and 5,6,7,8-tetrahydronaphthalene-1-yl group was favored to the biological activities from our previous report. [20] So these important fragments were also employed at R^1 position in our initial design of oral drug. To improve the metabolic stability, the hydrogen and methoxy methene groups were designed at R^2 position. With the same substituents at R^2 position, exploration of R^1 substituents revealed the following activity orders: (1) for the methoxy methene group at R^2 position, 5,6,7,8-tetrahydronaphthalene-1-yl (**5b**, 4.82 nM) > 2,5-dichlorobenz-yl (**5c**, 8.21 nM) > pyrazin-2-yl (**5a**, 74.86 nM); (2) for H atom at R^2 position, 5,6,7,8-tetrahydronaphthalene-1-yl (**5e**, 5.89 nM) > 2,5-dichlorobenz-yl (**MLN2238**, 7.73 nM) > pyrazin-2-yl (**5d**, 303.8 nM). These data indicated that 2,5-dichlorobenz-yl and 5,6,7,8-tetrahydronaphthalene-1-yl fragments were more beneficial to activities than pyrazin-2-yl, which was consistent with our previous study that hydrophobic groups were preferred for R^1 position.[21]

In our previous reports,[22-26] several aromatic groups at R^1 position of compounds were synthesized and biologically evaluated. However, aliphatic groups at R^1 position had never been studied. To fully understand SAR of dipeptidyl boronates, several aliphatic groups at R^1 position were designed including straight chain and cyclic fragments. Firstly, with the H atom substitution at R^2 position, compounds with the aliphatic groups at R^1 position were designed to investigate the activities and the results showed that the potency was significantly reduced compared with **MLN2238**. Results of cyclization with three, four or six membered rings at R^1 position showed that bigger ring was more potent than smaller one, such as cyclohexyl (**5h**, 12.89 nM) > cyclobutyl (**5g**, 21.17 nM) > cyclopropyl (**5f**, 387.0 nM). As to the straight

chain substituents at R^1 position, the biological results showed that longer straight chains were beneficial to the activities. Compared with propyl substituted compound **5j** (42.79 nM), butyl **5k** (30.78 nM) and pentyl **5l** (27.75 nM), the activity of the shortest ethyl **5i** (593.7 nM) was decreased by 14, 19 and 21 folds, respectively. Furthermore, the branched aliphatic chain (isobutyl compound **5m**, 20.44 nM) was more potent than the straight one (butyl **5k**, 30.78 nM). However, too much bulky fragment 2,2-dimethylbutyl **5n** (26.79 nM) reduced the potency compared with isobutyl compound **5m** (20.44 nM).

Secondly, for the phenyl fragment at R^2 position, aromatic groups were substituted by aliphatic straight chain groups at R^1 position (compounds **5o**-**5v**) to investigate the activities. The results indicated that the activities of the straight chain compounds, such as butyl (**5p**, 3.53 nM), pentyl (**5q,** 2.31 nM), hexyl (**5r**, 1.98 nM) and isobutyl (**5s**, 4.16 nM) were more active than **MLN2238** (7.73 nM). But the smallest ethyl (**5o**, 8.11 nM) was an exception. Interestingly, when the length of straight chain of R^1 group was increased, the activities were increased. Furthermore, results of cyclization with three, four or six membered rings at R^1 position showed that the bigger ring was more potent than the smaller one, such as cyclohexyl (**5v**, 3.22 nM) > cyclobutyl (**5u**, 5.26 nM) > cyclopropyl (**5t**, 8.86 nM). The biological data suggested that phenyl group was more potent than H atom at the R^2 position when aliphatic groups were substituted at the R^1 position. However, the phenyl group at R^2 position was not stable in the microsome metabolism experiments (data not shown). It was reported that the prodrug **MLN9708** could rapidly hydrolyzes to its biologically active form boronic acid **MLN2238** in aqueous solutions and both forms had similar activities.[22] So in this manuscript, more stable methoxy methene group was introduced at R^2 position of our novel orally available compound **5c** and converted to its prodrug **6a** (6.74 nM), which was as potent as its biologically active form **5c**. The selectivity results showed that compound **6a**, **Bortezomib** and **MLN9708** were also active against β1 subunit and were nearly inactive to inhibit β2 subunit.

2.2.2. Cell

The marketed drug **MLN9708** was approved for the treatment of multiple

myeloma in 2015. In this manuscript, we evaluated the cytotoxic potentials of compounds against three multiple myeloma cell lines, RPMI8226, ARH77 and U266B. The compounds with the IC_{50} values of enzymatic inhibition less than 10 nM were further investigated to evaluate their potential antitumor activities in cancer cell lines. The cellular activities of these compounds, **bortezomib, MLN2238** and **MLN9708** were displayed in Table 2.

Table 2

The cellular activities of compounds against MM cell lines (IC_{50}, nM)

Compd.	RPMI8226	U266B	ARH77
5b	32.78	15.09	14.41
5c	8.99	6.75	9.10
5o	13.25	12.26	9.51
5p	6.00	5.22	5.12
5q	6.03	4.88	5.32
5r	31.04	96.22	20.55
5s	5.51	5.28	4.70
5t	18.94	14.17	10.34
5u	10.31	5.46	6.07
5v	11.93	5.97	7.59
6a	2.59	4.32	3.68
bortezomib	11.20	11.63	9.57
MLN2238	55.32	52.15	65.50
MLN9708	49.74	67.10	43.25

In general, all the compounds showed significant inhibitory potency against

RPMI8226, ARH77 and U266B multiple myeloma cell lines compared with the standards. Especially, the compounds with 2,5-dichlorobenz-yl (**5c** and **6a**) and the aliphatic chain groups (**5p**, **5q** and **5s**) at R^1 positions displayed strong antiproliferative activities with the IC_{50} values less than 10 nM. However, compounds **5o-5v** were substituted by the hydrophobic aliphatic groups at the R^1 position and were poorly soluble and not suitable for drug candidates. Prodrug **6a**, which was substituted with methoxy methene group at R^2 position, was selected for the next study of microsomal stabilities.

2.2.3. Microsomal stabilities

The microsomal stabilities of prodrug **6a** were determined with various species of liver microsomes, such as rat, mice, dog, monkey and human and the results were illustrated in Table 3. The marketed **MLN9708** was selected as the standard. The half-life ($T_{1/2}$) and intrinsic clearance (CL_{int}) data were used to evaluate the metabolic stabilities. The results indicated that the half-lives of compound **6a** in mice and dog species were nearly close to **MLN9708**. While in rat species, the half-life of compound **6a** was longer than **MLN9708**, which indicated that it was metabolized more slowly than **MLN9708** and on the contrary, compound **6a** was metabolized more quickly than **MLN9708** in monkey and human species.

Table 3

The microsomal stabilities of compounds **6a** and **MLN9708**

Compd.	Parameters	Species				
		Rat	Mice	Dog	Monkey	Human
6a	$T_{1/2}$ (min)	76.9	33.9	74.9	15.6	31.1
	CL_{int} (mL/min/kg)	18.0	40.8	18.5	88.8	44.5
MLN9708	$T_{1/2}$ (min)	46.2	30.1	69.3	33	63
	CL_{int} (mL/min/kg)	30.0	46.0	20.0	42.0	22.0

2.2.4. Pharmacokinetic studies

Compound **6a** was further investigated by profiling iv and ig pharmacokinetics in male Sprague-Dawley (SD) rats. The pharmacokinetics parameters were listed in

Table 4. The results illustrated that the elimination phase half-lives of compound **6a** were 5.28 h for ig and 0.4 h for iv, respectively. The oral bioavailability of compound **6a** was 24.9%, which was nearly equal to **MLN2238** (27.8%)[27] and could be a drug candidate to develop.

Table 4

Single dose iv and ig pharmacokinetic profiles of **6a** in SD rats

Compd.		Dose(mg/kg)	$T_{1/2}$(h)	AUC_{last}(h*ng/ml)	MRT_{last}(h)	Vz_obs	Cl_obs	F
6a	ig[a]	1.2	5.28	883	5.37	-	-	24.9%
	iv[b]	0.2	0.4	591	3.68	201.3	341.1	

[a] ig, intragastric administration; [b] iv, intravenous injection.

2.2.5. Mouse tumor xenograft efficacy study

Compound **6a** was further evaluated for in vivo antitumor efficacy using xenograft mouse model of ARH77. Female nude mice bearing ARH77 tumor were dosed orally with **MLN9708** and compound **6a** over a 21-day period and the results were shown in Figure 2. The results showed that compound **6a** displayed significant in vivo antitumor efficacy and induced tumor stasis. Dosing at 1 mg/kg daily of compound **6a**, the tumor volume was reduced significantly compared with the vehicle and **MLN9708** with the treatment of 5 mg/kg twice a week. In addition, compound **6a** was well-tolerated and no mortality or significant loss of body weight was observed during treatment. The tumor growth values (T/C%) of **MLN9708** and compound **6a** were 160.02% and 392.41% at two different doses, respectively. And the tumor growth inhibition values (TGI%) were 33.11% and 81.74%, respectively (Table 5).

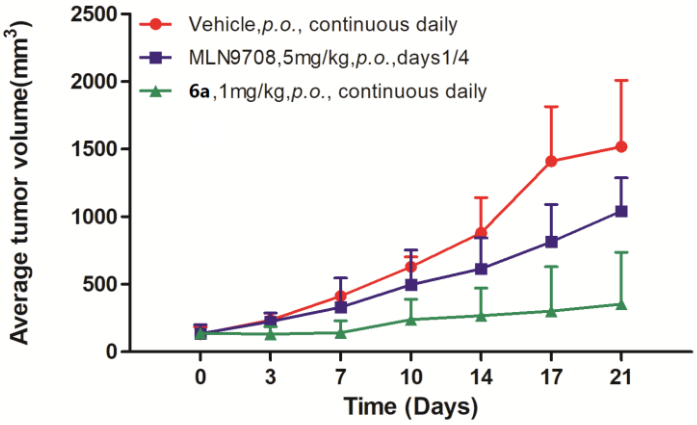

Figure 2. Antitumor activities of compounds **6a** and **MLN9708** in mice bearing human ARH77 MM tumor xenografts.

Table 5

In vivo antitumor effects of compounds **6a** and **MLN9708** in human ARH77 xenograft nude mouse model

Groups	TV [b] Mean (mm^3)	RTV [c] Mean	T/C [d] (%)	RTV SF [e]	TW [f] Mean (Day 21, g)	TGI [g] (%)
Control (PBS) [a]	1518.82	10.04			1.78	-
MLN9708 (5 mg/kg）	1042.71	9.13	63.69%		1.33	33.11%
6a (1 mg/kg)	354.78	3.72	25.36%	*	0.65	81.74%

[a] PBS: phosphate buffer saline; [b] TV: tumor volume; [c] RTV: relative tumor volume, the individual RTV was calculated as follows: RTV = V_t/V_0, where V_0 is the volume on the day of initial treatment and V_t is the volume on each day of measurement; [d] T/C=$RTV_{treatment}/RTV_{control}$ 100%; [e] SF: statistical significance (*p<0.05); [f] TW: tumor weight; [g] TGI: tumor growth inhibition, TGI (%) = ($TW_{control}$-$TW_{treatment}$)/$TW_{control}$ 100%.

2.2.6. Cell cycle

Mechanism studies were carried out to understand how compound **6a** stopped the progression of cancer cells. The cell cycle distributions of U266B cells treated with DMSO and compound **6a** were shown in Figure 3A and 3B, respectively. The results showed that compound **6a** significantly arrested cancer cells in the G2/M phase of the cell cycle with an obvious decrease in the proportion of cells in the G0/G1 phase in

comparison with control cells. After treatment with compound **6a**, the cancer cell percentage of G2/M phase was 21.90%, compared with 12.33% of the solvent control. The results indicated that compound **6a** could inhibit the growth of cancer cells by inhibiting the cell cycle progression.

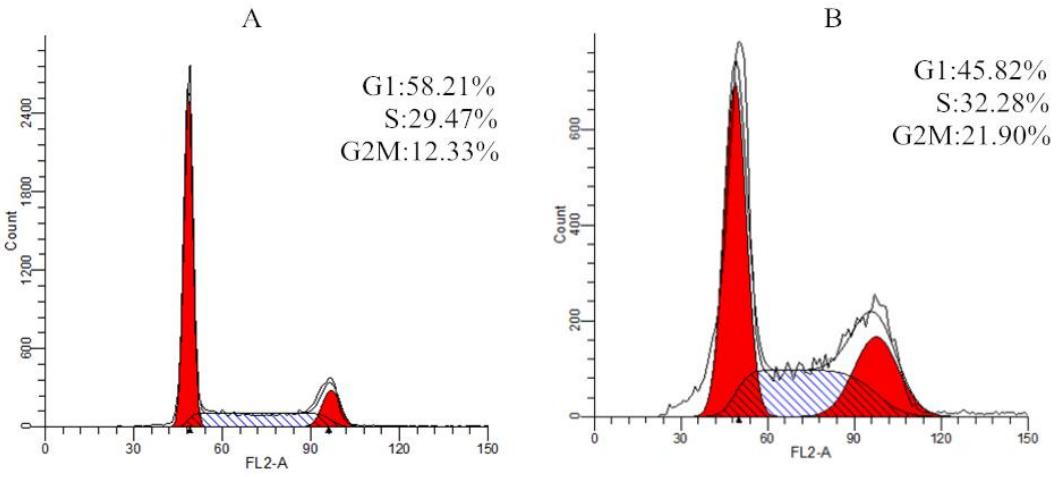

Figure 3. Cell cycle profiles of U266B cells treated with (A) DMSO, 15 nM of (B) compound **6a**.

3. Conclusion

A series of novel dipeptidyl boronic acid proteasome inhibitors constructed by α-amino acids were designed, synthesized and biologically investigated in vitro and in vivo by varying different substituents at R^1 and R^2 positions of the backbone. Aliphatic groups at R^1 position were synthesized to fully understand the SAR. Among the screened inhibitors, compound **5c** showed the most potent activity in inhibiting the proteasome and almost the same cellular activities as the standard **MLN2238**. To investigate the oral availability, compound **5c** was then esterified to its prodrug **6a**, which exhibited good pharmacokinetic properties. Metabolic stabilities indicated that prodrug **6a** showed good microsomal stabilities. In vivo efficacy of compound **6a** in ARH77 mouse xenograft tumor model showed that the tumor volume was significantly reduced compared with the control group and no serious side effects were observed. The mechanism study showed that compound **6a** had a significant inhibitory effect on CT-L activity and stopped the cell cycle progression at G2/M stage. With the data in hand, prodrug **6a** was selected as a clinical candidate to develop.

4. Experimental section

4.1. Chemistry

Unless otherwise stated, commercial reagents were used directly without any purification, and all solvents were dried by standard methods before using. Yields refer to chromatographically and were not optimized unless otherwise stated. Reactions were monitored by thin-layer chromatography on precoated silica gel GF254 plates and the spots were tested under 254 nm UV light, 10% ethanolic phosphomolybdic acid, 20% n-butyl alcoholic ninhydrin heat as developing agent. HPLC showed purity of all the final products was greater than 95%. Melting points were determined on an YRT-3 melting point apparatus. ^{1}H NMR and ^{13}C NMR spectra were recorded at room temperature on a Bruker ARX400 spectrometers using TMS as an internal standard. Chemical shifts were reported in ppm (δ units) and coupling constants (J) were expressed in hertz. The following abbreviations were used to designate the multiplicities as s (singlet), d (doublet), t (triplet), q (quartet), dd (doublet of doublets) and m (multiplet). Mass spectra were recorded on Thermo Fisher LC-MS instruments in electrospray positive and negative ionization modes. High-resolution mass spectra (HRMS) were recorded on a ZAB-HS instrument using an electrospray source (ESI).

4.1.1. (S)-2-amino-3-methoxy-N-((R)-3-methyl-1-((3aS,4S,6S,7aR)-3a,5,5-trimethyl hexahydro-4,6-methanobenzo[d][1,3,2]dioxaborol-2-yl)butyl)propenamide hydrochloride (3a)

To a cooled solution (-10 °C) of (S)-N-boc-2-amino-3-methoxy-propionic acid (4.73 g, 21.58 mmol) dissolved in anhydrous CH_2Cl_2 (120 mL) was added HOBt (4.38 g, 32.37 mmol). After 10 min, EDCI (6.2 g, 32.37 mmol) was added. Finally, intermediate **5** (8.19 g, 21.58 mmol) and DIPEA (9.77 g, 75.53 mmol) were added. The mixture was stirred at -10 °C for 1 h and at room temperature for 15 h. The mixture was washed with 10% hydrochloric acid, 5% $NaHCO_3$ and brine, respectively and dried over anhydrous Na_2SO_4. After filtration and evaporation, the obtained crude

product was directly used in the next reaction.

The prepared boric acid ester was dissolved in ethyl acetate (30 mL) and was dropwise added 4.5 mol/L HCl in ethyl acetate (55 mL) at 0 °C. Then the mixture was stirred for 2 h at room temperature and the ethyl acetate was evaporated under vacuo. MTBE was added to the residue and filtered to obtain glassy solid **3a** (7.8 g, 89.7%). ^{1}H NMR (400 MHz, DMSO) δ 0.81 (s, 2H), 0.85 (dd, J_1 = 3.7 Hz, J_2 = 6.5 Hz, 6H), 1.16-1.23 (m, 2H), 1.24 (s, 3H), 1.31 (s, 3H), 1.41-1.49 (m, 1H), 1.60-1.74 (m, 2H), 1.80-1.86 (m, 1H), 1.92 (dd, J_1 = 4.1 Hz, J_2 = 9.7 Hz, 1H), 2.07-2.16 (m, 1H), 2.22-2.31 (m, 1H), 2.91-3.01 (m, 1H), 3.27 (s, 3H), 3.58-3.68 (m, 2H), 3.94-4.05 (m, 1H), 4.27 (dd, J_1 =1.8 Hz, J_2 = 8.7 Hz, 1H), 8.32 (d, J = 3.8 Hz, 3H), 8.71 (dd, J_1 = 6.0 Hz, J_2 = 13.6 Hz, 1H). MS (ESI) m/z 367.6 $[M+H]^+$.

4.1.2. 2,5-dichloro-N-((S)-3-methoxy-1-(((R)-3-methyl-1-((3aS,4S,6S,7aR)-3a,5,5-Trimethylhexahydro-4,6-methanobenzo[d][1,3,2]dioxaborol-2-yl)butyl)amino)-1-oxopropan-2-yl)benzamide (4c)

To a cooled solution (-10 °C) of 2,5-dichlorobenzoic acid (0.53 g, 2.75 mmol) dissolved in anhydrous CH_2Cl_2 (30 mL) was added HOBt (0.56 g, 4.13 mmol). After 10 min, EDCI (0.79 g, 4.13 mmol) was added. Finally, intermediate (aR,3aS,4S,6S,7aR)-Hexahydro-3a,8,8-trimethyl-alpha-(2-methylpropyl)-4,6-methan o-1,3,2-benzodioxaborole-2-methanamine 2,2,2-trifluoroacetate (1.11 g, 2.75 mmol) and DIPEA (1.24 g, 9.63 mmol) were added. The mixture was stirred at -10 °C for 1 h and at room temperature overnight. The mixture was washed with 1N HCl, 5% $NaHCO_3$, and brine, respectively and dried over anhydrous Na_2SO_4. After filtration, evaporation and purification with chromatography (petroleum ether/EtOAc = 3:1), 1.2 g (80.8%) of glassy solid was obtained. ^{1}H NMR (400 MHz, $CDCl_3$) δ 0.79-0.90 (m, 3H), 0.90-0.94 (m, 6H), 1.17-1.27 (m, 2H), 1.29 (s, 3H), 1.38 (s, 3H), 1.46-1.52 (m, 1H), 1.57-1.68 (m, 1H), 1.79-1.95 (m, 2H), 1.98-2.05 (m, 1H), 2.14-2.23 (m, 1H), 2.28-2.37 (m, 1H), 3.27-3.37 (m, 1H), 3.41 (s, 3H), 3.46-3.53 (m, 1H), 3.92 (dd, J_1 = 4.0 Hz, J_2 = 9.0 Hz, 1H), 4.26-4.35 (m, 1H), 4.65-4.73 (m, 1H), 6.41-6.74 (m, 1H), 7.11-7.23 (m, 1H), 7.30-7.37 (m, 2H), 7.64 (d, J = 7.4 Hz, 1H). MS (ESI) m/z 539.4 $[M+H]^+$.

4.1.3.

((R)-1-((S)-2-(2,5-dichlorobenzamido)-3-methoxypropanamido)-3-methylbutyl) boronic acid (5c)

To the solution of boronic acid ester **4c** (1.1 g, 2.17 mmol) and isobutyl boronic acid (1.1 g, 10.9 mmol) dissolved in methanol (15 mL) and hexane (15 mL) was added 1 N HCl (5 mL). The mixture was stirred at room temperature for 22 h. The methanolic phase was washed with hexane (3 × 15 mL), and the hexane layer was extracted with methanol (15 mL). The combined methanolic layers were evaporated in vacuo, and the residue was dissolved in CH_2Cl_2 (10 mL). The solution was washed with brine (3 × 10 mL), and the organic layer was dried over anhydrous Na_2SO_4, evaporated, and purified with chromatography to give 0.61 g of white foam solid **5c** (69.8%). ^{1}H NMR (400 MHz, $CDCl_3$) δ 0.84-0.89 (m, 3H), 0.89-0.93 (m, 3H), 1.30-1.54 (m, 2H), 1.54-1.67 (m, 1H), 3.40 (s, 3H), 3.51-3.65 (m, 2H), 3.87-3.94 (m, 1H), 4.62-4.93 (m, 1H), 7.29-7.37 (m, 2H), 7.56-7.65 (m, 1H). ^{13}C NMR (100 MHz, $CDCl_3$) δ 22.87, 25.79, 39.73, 53.20, 59.05, 59.12, 71.15, 129.03, 129.77, 131.32, 133.07, 135.55, 165.34, 172.18. MS (ESI) m/z 403.0 $[M-H]^-$. HRMS (ESI) calcd for $C_{16}H_{23}BCl_2N_2NaO_5$ $[M+Na]^+$, 427.0972; found, 427.0974.

4.1.4. N-((S)-1-(((R)-1-(1,3,6,2-dioxazaborocan-2-yl)-3-methylbutyl)amino)-3-methoxy-1-oxopropan-2-yl)-2,5-dichlorobenzamide (6a)

To the solution of diethanolamine (0.07 g, 0.82 mmol) dissolved in ethyl acetate (5 mL) at 74 °C was added dropwise the solution of boronic acid **5c** (0.3 g, 0.74 mmol) dissolved in ethyl acetate (1 mL) and then cooled slowly to 60 °C. The mixture was stirred at 60 °C for 3 h. The resulting slurry was cooled slowly to room temperature and the mixture was stirred overnight. The mixture was filtered and the white solid **6a** was obtained (0.23 g, 65.6%). ^{1}H NMR (400 MHz, DMSO) δ 0.80 (dd, J_1 = 6.7 Hz, J_2 = 9.7 Hz, 6H), 1.12 -1.39 (m, 2H), 1.59 (d, J = 5.5 Hz,1H), 2.75 (dd, J_1 = 6.4 Hz, J_2 = 26.3 Hz, 2H), 2.85-3.04 (m, 2H), 3.08-3.20 (m, 1H), 3.26 (s, 3H), 3.59 (dd, J_1 = 8.1 Hz, J_2 = 22.2 Hz, 4H), 3.69 (d, J = 5.3 Hz, 2H), 4.59 (dd, J_1 = 6.7 Hz, J_2 = 12.9 Hz,1H), 6.56 (s, 1H), 6.99 (d, J = 8.2 Hz, 1H), 7.45 (d, J = 13.7 Hz, 1H), 7.54 (s, 2H), 8.69-8.82 (m, 1H). ^{13}C NMR (100 MHz, DMSO) δ 21.59, 23.97, 24.44, 50.51, 50.83,

53.43, 58.07, 62.43, 71.74, 128.58, 130.64, 131.38, 131.48, 137.83, 164.86, 168.15. HRMS (ESI) calcd for $C_{20}H_{30}BCl_2N_3NaO_5$ $[M+Na]^+$, 496.1656; found, 496.1659.

4.2. Enzyme inhibition assays

The enzymatic activities of the proteasome were analyzed using fluorogenic peptides: Suc-Leu-Leu-Val-Tyr-AMC (Suc represents succinyl and AMC represents 7-amido-4-methyicoumarin, obtained from Enzo) for chymotryptic-like (CT-L) activity. Four microliter of human 20S proteasome (0.2 nM) was hatched with 4 μl various concentrations of compounds. After 10 min, 8 μL of fluorogenic peptides (50 μM) was added and incubated at 37 °C for 1 h. The fluorescence of released AMC reagents, was measured by a spectrofluorimeter (CLARIOstar, BMG Germany) at excitation and emission wavelengths of 360/460 nm. 1% DMSO was served as solvent control. An inhibition rate was calculated and then the IC_{50} value was inferred compared with the fluorescence of solvent control.

4.3. Cell culture and cytotoxicity assays

The cytotoxic effects of compounds were detected using CellTiter 96 Aqueous One Solution Cell Proliferation assay (Promega). Suspension cells (RPMI8226, ARH77, U266B) growing in log phase were plated at 5000-10000 cells per well. U266B cells were plated at 10000 cells per well and collected by centrifugation, while the other two at 5000 cells. Twenty-four hours after plating, media including the test compounds were added to each well to afford the intended final concentration. After 72 h, the cells' viability was detected using the assay protocol recommended by the manufacturers. The resulting signals were quantified using a CLARIOstar Microplate Reader (BMG LABTECH).[28]

4.4. Cell cycle

DNA content distribution of cellular population was measured by flow cytometry. To determine whether the cells treated with drug made cycle arrest, cells were harvested, centrifuged and washed thrice with phosphate-buffered saline. The supernatant was removed and each sample in tube was added 300 μL of resuspended cells. Cells were fixed in 700 μL of precooled anhydrous ethanol at -20 °C overnight, and then centrifuged and washed twice with phosphate-buffered saline again after

anhydrous ethanol removed. Cells were counted and 500 μL of PI/RNase Staining Buffer (BD company) were added in about 3~5 × 10^5 cells and resuspended. The solution was stained at 4 ℃ for 20 min in dark place. The cells were then analyzed with flow cytometry (FACSCailbur). The cell cycle distribution was presented as the percentage of cells containing.[29]

4.5. Pharmacokinetic studies

Compound **6a** was given by gavage at a dose of 1 mg/kg and caudal intravenously at a dose of 0.2 mg/kg. Orbital blood was collected at 0 min, 2 min, 5 min, 15 min, 30 min, 1 h, 2 h, 4 h, 8 h, 12 h, 24 h and 30 h after oral administration, and at 0 min, 2 min, 5 min, 15 min, 30 min, 1 h, 2 h, 4 h, 8 h, 12 h, 24 h after tail intravenous administration. The blood samples were centrifuged at 3500 rpm for 10 min to obtain the plasma fraction, and 200 μL of plasma was stored at -25 ℃ until analysis. The drug concentration in the plasma were quantitatively analyzed using liquid chromatography-tandem mass spectrometry method (LC-MS/MS). Pharmacokinetic parameters were determined by a non-compartmental analysis using WinNonlin 6.3 program.

4.6. Liver microsomal stabilities

The elimination half-lives of compounds **6a** and **MLN9708** were calculated by monitoring the remaining percentages at different time points of the test compounds in liver microsomes (rat, mice, dog, monkey and human liver microsomes). A typical incubation mixture (300 μL total volume) for metabolic stability studies contained 0.1 mM phosphate buffer saline, 1 mM NADPH, 5 mM $MgCl_2$, 0.5 mg/mL microsomal protein and 1 μM test compounds. After preincubation at 37 ℃ for 5 min, the reactions were started by addition of NADPH and further incubated for another 0, 10, 20, 30, 60 min. And for the control experiments, liver microsomes and/or NADPH were omitted from these incubations. The reactions were terminated by adding methyl alcohol containing tolbutamide (100 ng/mL) as internal standard and keeping on ice for 30 min, followed by centrifugation at 4 ℃, 4000 rpm for 20 min to obtain the supernatant. Aliquots (5 μL) were then analyzed for substrate disappearance using liquid chromatography tandem mass spectrometry (Shimadzu company LC-20AD

HPLC instrument and ABSciex API4000) equipped with an electrospray ion source.[28]

4.7. Mouse tumor xenograft efficacy study

ARH77 xenograft model was established by 1×10^7 cells subcutaneously inoculated in female nude mice about 4-6 weeks of age at the time of tumor challenge. Upon the tumors were touchable, mice were randomized to treatment groups and treated orally with vehicle (5% HPβCD) or **MLN9708** (5 mg/kg) on a twice weekly schedule for 3 weeks or compound **6a** (1 mg/kg) daily for 21 days. Data were presented as mean tumor volume ± SD. (n=5/group).

Acknowledgments

This work was supported by the following grants: Natural Science Foundation of Jiangsu Province (No. BK20171448), National and Local Joint Engineering Research Center of Biomedical Functional Materials and Priority Academic Program Development of Jiangsu Higher Education Institutions (PAPD).

Supporting information

Characterization data for compounds 3b-3c, 4a-4v and 5a-5v.

Detailed procedures for all final compounds and the other key intermediates; MS and NMR spectrum for all final compounds; HRMS analysis data for all final compounds.

Abbreviations used

SAR, structure-activity relationship; UPP, ubiquitin-proteasome pathway; FDA, Food and Drug Administration; ATP, Adenosine triphosphate; CP, core particle; RP, regulatory proteasome; C-L, caspase-like; T-L, trypsin-like; CT-L, chymotrypsin-like; EDCI, 1-ethyl-3-(3-dimethylaminopropyl)-carbodiimide hydrochloride; HOBt, 1-hydroxybenzotriazole; DIPEA, N,N-diisopropylethylamine; IC_{50}, half-maximum inhibitory concentration; $T_{1/2}$, half-life; AUC, area under the curve; SD, Sprague-Dawley; NMR, nuclear magnetic resonance; MS, mass spectrometry; HRMS,

high resolution mass spectrometry.

References and notes

1. Goldberg, A. L. *Nature* **2003**, *426*, 895.

2. Tsukamoto, S.; Yokosawa, H. *Curr. Med. Chem.* **2006**, 13, 13745.

3. Chen, J. J.; Lin, F., Qin, Z. H. *Neurosci. Bull.* **2008**, 24, 183.

4. Ciechanover, A. *Biochem. Soc. T.* **2003**, 31, 474.

5. Borissenko, L.; Groll, M. *Chem. Rev.* **2007**, 107, 687.

6. Lander, G. C.; Estrin, E.; Matyskiela, M. E; Bashore, C.; Nogales, E.; Martin, A. *Nature* **2012**, 482, 186.

7. Coux, O.; Tanaka, K.; Goldberg, A. L. *Annu. Rev. Biochem*. **1996**, 65, 801.

8. Groll, M.; Ditzel, L.; Lowe, J.; Stock, D.; Bochtler, M.; Bartunik, H. D.; Huber, R. *Nature* **1997**, 386, 463.

9. Herrmann, J.; Ciechanoverb, A.; Lermanc, L. O.; Lerman, A. *Cardiovasc. Res.* **2004**, 61, 11.

10. Mani, A.; Gelmann, E. P. *J. Clin. Oncol*. **2005**, 23, 4776.

11. Ciechanover, A.; Brundin, P. *Neuron* **2003**, 40, 427.

12. Richardson, P. G.; Sonneveld, P.; Schuster, M. W.; Irwin, D.; Stadtmauer, E.A.; Facon, T.; Harousseau, J. L.; Yehuda, B. D.; Lonial, S.; Goldschmidt, M. B.; Cavenagh, J.; Dalton, W. S.; Boral, A. L.; Esseltine, D. L.; Porter, J. B.; Schenkein, D.; Anderson, K. C. *N. Engl. J. Med.* **2005**, 352, 2487.

13. O´Connor, O. A. Clin. *Lymphoma Myeloma* **2005**, 6, 191.

14. Fisher, R. I.; Bernstein, S. H.; Kahl, B. S.; Djulbegovic, B.; Robertson, M. J.; de Vos, S.; Epner, E.; Krishnan, A.; Leonard, J. P.; Lonial, S.; Stadtmauer, E. A.; O'Connor, O. A.; Shi, H.; Boral, A. L.; Goy, A. *J. Clin. Oncol.* **2006**, 24, 4867.

15. Bakas, N. A.; Schultz, C. R.; Yco, L. P.; Roberts, C. C.; Chia-en, A. C.; Bachmann, A. S.; Pirrung, M. C. *Bioorg. Med. Chem.* **2018**, 26, 401.

16. Totaro, K. A.; Barthelme, D.; Simpson, P. T.; Sauerb, R. T.; Selloet, J. K. *Bioorg. Med. Chem.* **2015**, 23, 6218.

17. Richardson, P. G.; Barlogie, B.; Berenson, J.; Singhal, S.; Jagannath, S.; Irwin, D.;

Rajkumar, S. V.; Srkalovic, G.; Alsina, M.; Alexanian, R.; Siegel, D.; Orlowski, R. Z.; Kuter, D.; Limentani, S. A.; Lee, S.; Hideshima, T.; Esseltine, D. L.; Kauffman, M.; Adams, J.; Schenkein, D. P.; Anderson, K. C. *N. Engl. J. Med*., **2003**, 348, 2609.

18. Chauhan, D.; Tian, Z.; Zhou, B.; Kuhn, D.; Orlowski, R.; Raje1, N.; Richardson, P.; Anderson, K. C. *Clin. Cancer Res.* **2011**, 17, 5311.
19. Supuran, C. T. *Bioorg. Med. Chem.* **2017**, 25, 5064.
20. Appel, A. *Nature* **2011**, 480, S40.
21. Kumar, S. K.; Bensinger, W. I.; Zimmerman, T. M.; Reeder, C. B.; Berenson, J. R.; Berg, D.; Hui, A.; Gupta, N.; Di Bacco, A.; Yu, J.; Shou, Y.; Niesvizky, R. P *Blood* **2014**, 124, 1047.
22. Lei, M.; Feng, H. Y.; Wang, C.; Li, H. L.; Shi, J. M.; Wang, J.; Liu, Z. G.; Chen, S. S.; Hu, S. H.; Zhu, Y. Q. *Bioorg. Med. Chem*. **2016**, 24, 2576.
23. Zhu, Y. Q.; Zhao, X.; Zhu, X. R.; Wu, G.; Li, Y. J.; Ma, Y. H.; Yuan, Y. X.; Yang, J.; Hu, Y.; Ai, L.; Gao, Q. Z. *J. Med. Chem*. **2009**, 52, 4192.
24. Zhu, Y. Q.; Lei, M.; Lu, A. J.; Zhao, X.; Yin, X. J.; Gao, Q. Z. *Eur. J. Med. Chem.* **2009**, 44, 1486.
25. Zhu, Y. Q.; Pei, J. F.; Liu, Z. M.; Lai L. H.; Cui, J. R.; Li, R. T. *Bioorg. Med. Chem.* **2006**, 14, 1483.
26. Zhu, Y. Q.; Yao, S. Y.; Xu, B.; G, Z. M.; Cui, J. R.; Cheng, T. M.; Li, R. T. *Bioorg. Med. Chem.* **2009**, 17, 6851.
27. Kupperman, E.; Lee, E. C.; Cao, Y. Y.; Bannerman, B.; Fitzgerald, M.; Berger, A.; Yu, J.; Yang, Y.; Hales, P.; Bruzzese, F.; Liu, J.; Blank, J.; Garcia, K.; Tsu, C.; Dick, L.; Fleming, P.; Yu, L.; Manfredi, M.; Rolfe, M.; Bolen, *J. Cancer Res*. **2010**, 70, 1970-1980.
28. Miller, Z.; Keun-Sik, K.; Do-Min, L.; Kasam, V.; Baek, S. E.; Lee, K. H.; Zhang, Y. Y.; Lin, A.; Carmony, K.; Na-Ra, L.; Zhou, S.; Zhao, Q. Q.; Jang, Y. J.; Hyun-Young, J.; Zhan, C. G.; Lee, W.; Kim, D. E.; Kim, K. *B. J. Med. Chem*. **2015**, 58, 2036.
29. Rastogi, N.; Mishra, D. P. *Cell Div*. **2012**, 7, 1.

Highlights

- Aliphatic groups at R^1 position were synthesized to fully understand the SAR.
- **6a** inhibited the CT-L activity and the MM cells RPMI8226, U266B and ARH77.
- **6a** showed almost the same bioavailability as **MLN2238**.
- **6a** inhibited cell cycle progression at the G2M stage.
- **6a** significantly inhibited tumor growth in a human ARH77 MM xenograft mouse model.

Graphical Abstract

Design, Synthesis, in Vitro and in Vivo Evaluation, and Structure-Activity Relationship (SAR) Discussion of Dipeptidyl Boronic Acid Proteasome Inhibitors as Anti-cancer Agents for the Treatment of Multiple Myeloma and Mechanism Studies

Meng Lei [a, 1], Huayun Feng [a, 1], Enhe Bai [b], Hui Zhou [b], Jia Wang [c], Jingmiao Shi [c], Xueyuan Wang [b], Shihe Hu [c, *], Zhaogang Liu [c], Yongqiang Zhu [b, *]

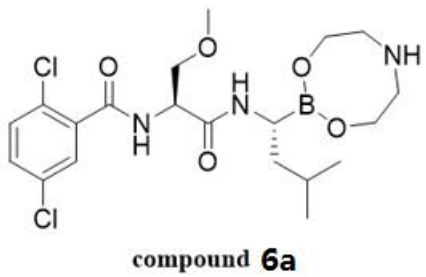

compound **6a**